

Comparison of the Cosserat Continuum Approach with Finite Element Interface Models in a Simulation of Layered Materials

A. Riahi^{1,*} and J.H. Curran²

Abstract. *This paper compares the formulation of the finite element Cosserat smeared approach with the combined finite element-explicit interface element approach, when both applied to the analysis of layered continua. The fundamental equations of both formulations are presented. Also, using three examples, the nature and accuracy of the displacement field predicted by both techniques are investigated and discussed.*

Keywords: *Cosserat theory; Layered continuum; Internal characteristic length; Transversely isotropic; Interface element; Finite element method.*

INTRODUCTION

The Cosserat continuum theory belongs to a group of enhanced or generalized continuum theories referred to as micropolar, gradient or directed continuum. The Cosserat theory was first proposed by the Cosserat brothers at the beginning of the past century [1]. However, some early attempts on generalized descriptions of continua can be traced back to the work of Voigt [2]. In the 1960s, theoretical aspects of gradient continuum theories were further developed by many researchers [3-5], but due to the lack of physical interpretation of micromoments and the unsymmetrical nature of stress, their application remained limited.

New interest in application of the Cosserat theory was initiated in the 1970s, by the work of Naghdi [6,7] on the theory of directed media. In the theory of directed media, motion of a 3-D continuum is described through a position vector, as well a number of director vectors, which represent the deformation of each material point. This approach has been applied with much success to the formulation of 3-D structural components such as shells, rods and points [8-13], where director vectors become physically interpretable.

Application of the Cosserat theory to the con-

tinuum description of materials with microstructure was initiated in the mid 1980s after a link was made between the Cosserat continuum description and localization analysis [14,15]. One of the first numerical applications of the Cosserat continuum description of materials with microstructures was in the analysis of the localization of shear bands in granular materials [16,17]. In recent years, the applicability of the Cosserat theory and the asymmetrical nature of stress in granular materials was a subject for discussion [18,19]. Also, application of the micropolar theory to the FEM formulation of layered and blocky materials was proposed [20-21] and was further extended to the numerical analysis of elastic, elasto-plastic and buckling problems in 2-D layered continua [22-26]. Application of the Cosserat theory to the 3-D analysis of materials with a layered microstructure has been limited in the past. Recently, the 2-D formulation was extended to simulate the behavior of 3-D layered materials [27-29]. Moreover, application of the Cosserat theory to the simulation of 2-D blocky materials, comparison of the Cosserat formulation for blocky materials with discrete methods [30,31] and recent extension to the 3-D analysis of masonry structures [32] suggest that the Cosserat-based FEM is mathematically rigorous. It is also physically meaningful for the analysis of materials with a periodical microstructure.

This paper focuses on application of the Cosserat continuum theory to the analysis of layered materials as an alternative to the classical continuum-based formulations that explicitly simulate the layers by utilizing

1. *Department of Civil Engineering, University of Toronto, Toronto, M5S 1A4, Canada*

2. *Rocscience Inc., 439 University Avenue, Toronto, M5G 1Y8, Canada.*

*. *Corresponding author. E-mail: a.riahi@utoronto.ca*

Received 23 June 2009; accepted 7 December 2009

specially devised interface elements. Interface surfaces represent the interaction condition at boundaries between materials, or interaction between two structural components such as plates or shells. Physically, such surfaces develop if the shear resistance at a surface is significantly lower than the shear resistance of the neighboring materials. From a mathematical point of view, an interface between two materials represents a discontinuity or jump in the displacement field and its derivatives (such as stress and strain). Interface elements formulate this jump by providing a relaxed connectivity in displacement of the nodes adjacent to their sides. Clearly, this approach restricts the size of the continuum elements used for the spatial discretization of layers to the layer thickness, which adds an unnecessary number of Degrees Of Freedom (DOFs) to the solution. Also, in three-dimensional analyses, geometric definition of arbitrarily-oriented layers, and further discretization of layers to a finite element mesh or a finite difference grid becomes increasingly complex.

This paper focuses on application of the Cosserat theory to the analysis of 2-D and 3-D layered continua. It is concerned with a class of problems where interface surfaces follow a sequential pattern, giving rise to new physical mechanisms due to the microstructure of the material, known as the internal length effects. In the Cosserat theory, each point of the continuum is associated with independent rotational degrees of freedom, in addition to the usual translational degrees of freedom. The basic kinematic variables of the Cosserat theory are displacements, first-order displacement gradients, microstructural rotations and rotation gradients. Higher-order displacement gradients are not considered. Consequently, in addition to normal and shear stains, rotational gradients develop within the continuum and, therefore, micromoments are required to define the kinematic-kinetic work conjugate pair. A direct consequence of introducing the new work conjugate pair is to relax stress tensor symmetry. The differences in the shear components of stress are equilibrated by micromoments. As a result, the Cosserat continuum theory provides a large-scale description of materials with microstructure, via additional kinematic and kinetic variables, and by introducing the physical (internal) length scale of a material into the governing equations of the system. For example, in the case of layered media, the bending stiffness of individual layers can be naturally incorporated into the constitutive equations, making the model different from conventional treatments.

The main objective of this paper is to compare the assumption and formulation of the finite element Cosserat solution to those of the finite element solution, which utilizes an interface element, and to investigate the accuracy and nature of the displacement field obtained from these solutions. Following this intro-

duction, the fundamentals of the Cosserat continuum, Cosserat rotations, and measures of strain and stress in the Cosserat continuum are discussed. Then, the 3-D FEM formulation of a Cosserat continuum and the constitutive equations of a 3-D stratified continuum are presented, respectively. Following that, the governing equations and the formulation of interface elements are briefly discussed. Finally, three numerical examples demonstrate the accuracy of the proposed FEM Cosserat formulation in the analysis of layered media.

COSSERAT CONTINUUM

Governing Equations, Micropolar Stress and Micropolar Couple Stress

The micropolar or Cosserat theory assumes that micromoments exist at each point of the continuum. In the Cosserat theory, the equilibrium of forces and moments in the current configuration are expressed in the following form [33]:

$$\sigma_{ij,i} + b_j = 0, \quad (1)$$

$$m_k + \mu_{k,j,j} + e_{kij}\sigma_{ij} = 0, \quad (2)$$

where \mathbf{b} is the body force, \mathbf{m} is the body couple moment, and $\boldsymbol{\sigma}$ and $\boldsymbol{\mu}$ are the Cosserat stress and Cosserat couple stress, or moment stress, respectively. The stress tensor, $\boldsymbol{\sigma}$, is analogous to the Cauchy stress of the classical continuum.

Also, the stress vector or stress traction and the couple stress vector or moment traction are defined by:

$$\mathbf{t}_\sigma = \boldsymbol{\sigma} \cdot \mathbf{n},$$

and

$$\mathbf{t}_m = \boldsymbol{\mu} \cdot \mathbf{n}, \quad (3)$$

where \mathbf{n} is the normal to the surface in the current or spatial configuration.

Figure 1 represents the stress and couple stress measures for a 3-D characteristic volume. The first subscript of the stress tensor refers to the direction of

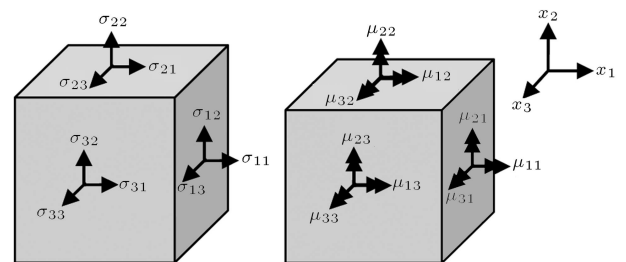


Figure 1. 3-D representation of stress and couple-stress measures.

the surface normal pertinent to the surface on which the stress acts. The second subscript of the stress refers to the direction in which the stress acts. The first subscript of the couple stress (or moment stress) refers to the axis about which it causes rotation, while the second subscript denotes the surface on which the moment stress acts. The notation adopted for stress tensor components is similar to the standard notation used in a classical continuum theory; however, it is different from the notation of some of the previous works on the Cosserat theory referred to in this paper [22-26]. The notation adopted for couple stress components is compatible with most literature on the Cosserat theory; however, it differs from the ordinary notation used in plate theory, where the moment subscript refers to the stress components by which the moments are produced (i.e., $M_x = \int_{-h/2}^{+h/2} \sigma_{xx} z dz$ [34]).

In the absence of body moment and when couple stress terms are self-equilibrated, the condition of symmetry of the Cauchy stress and its work conjugate strain measure is retrieved, and the Cosserat continuum reduces to the classical continuum.

Infinitesimal and Finite Cosserat Rotations

Compared to a classical continuum, an enhanced or Cosserat continuum is obtained by adding a rotation, \mathbf{R}^c , to each point of the continuum. A Cosserat rotation is defined as the independent rotation of a rigid triad attached to each material point, which rotates independently with respect to the material triad. The representation of micropolar rotation, in its most general form, is given by [35]:

$$\mathbf{R}^c = \exp(\text{spn}(\boldsymbol{\theta}^c)), \quad (4)$$

where $\boldsymbol{\theta}^c$ is the axial vector of rotation, or the independent rotation vector, and defines the axis of rotation with rotation angle θ^c . The rotation vector, $\boldsymbol{\theta}^c$, can be expressed by:

$$\boldsymbol{\theta}^c = \theta_i e_i, \quad (5)$$

where e_i is the i th component of the base vector. Rotation angle θ^c is defined as:

$$\theta^c = \|\boldsymbol{\theta}^c\|. \quad (6)$$

The skew symmetric tensor associated with the axial vector is expressed by:

$$\text{spn}(\boldsymbol{\theta}^c) = \mathbf{e} \cdot \boldsymbol{\theta}^c, \quad (7)$$

where \mathbf{e} is the permutation symbol and, thus Equation 7 can be expressed in the following matrix form:

$$\text{spn}(\boldsymbol{\theta}^c) = \begin{pmatrix} 0 & -\theta_3 & \theta_2 \\ \theta_3 & 0 & -\theta_1 \\ -\theta_2 & \theta_1 & 0 \end{pmatrix}. \quad (8)$$

The mathematical definition of the rotation tensor, \mathbf{R}^c , is [35]:

$$\begin{aligned} \mathbf{R}^c &= \exp(\text{spn}(\boldsymbol{\theta}^c)) = \cos(\theta^c) \mathbf{I} + \frac{\sin(\theta^c)}{\theta^c} \text{spn}(\boldsymbol{\theta}^c) \\ &\quad + \frac{1 - \cos(\theta^c)}{(\theta^c)^2} \boldsymbol{\theta}^c \otimes \boldsymbol{\theta}^c. \end{aligned} \quad (9)$$

The above formula represents the finite rotation of a generalized continuum. In most cases, its terms are not closed-form. One exception is when rotation vector $\boldsymbol{\theta}^c$ coincides with one of the coordinate directions. When $\boldsymbol{\theta}^c$ coincides with e_3 , for example, the terms of Equation 9 can be expressed as:

$$\mathbf{R}^c = \begin{pmatrix} \cos(\theta_3) & -\sin(\theta_3) & 0 \\ \sin(\theta_3) & \cos(\theta_3) & 0 \\ 0 & 0 & 1 \end{pmatrix}. \quad (10)$$

In a small rotation framework, the rotation matrix, \mathbf{R}^c , is approximated (using series expansion) by the following:

$$\mathbf{R}^c \cong \mathbf{I} + \text{spn}(\boldsymbol{\theta}) = \begin{pmatrix} 1 & -\theta_3 & \theta_2 \\ \theta_3 & 1 & -\theta_1 \\ -\theta_2 & \theta_1 & 1 \end{pmatrix}. \quad (11)$$

Micropolar Strain and Curvature

A comprehensive study of the micropolar theory of finite rotations and finite strains has been conducted by Steinmann [35]. Using the principle of virtual work (Equations 1 and 2), it can be shown that the work conjugate measure of strain to $\boldsymbol{\sigma}$, is defined as follows:

$$\gamma_{ij} = u_{j,i} - e_{ijk} \theta_k, \quad (12)$$

where e_{ijk} is the permutation symbol.

In a Cosserat continuum, in addition to the rotation of the rigid triad, with respect to the material (reference) triad, which is defined as the Cosserat rotation, variation in rotations of adjacent triads is another kinematic variable that is introduced in the formulation, and which is referred to as curvature. Curvature is a third-order anti-symmetric tensor, and can be reduced to a second-order tensor as:

$$\kappa_{ls} = \frac{1}{2} (e_{lij} R_{ki}^c R_{kj,s}^c). \quad (13)$$

By substituting \mathbf{R}^c (Equation 11) into the above expression, and by disregarding any higher-order terms of rotation, the expression for the second-order curvature tensor becomes:

$$\boldsymbol{\kappa} = \begin{pmatrix} \kappa_{11} & \kappa_{12} & \kappa_{13} \\ \kappa_{21} & \kappa_{22} & \kappa_{23} \\ \kappa_{31} & \kappa_{32} & \kappa_{33} \end{pmatrix} = \begin{pmatrix} -\theta_{1,1} & -\theta_{1,2} & -\theta_{1,3} \\ -\theta_{2,1} & -\theta_{2,2} & -\theta_{2,3} \\ -\theta_{3,1} & -\theta_{3,2} & -\theta_{3,3} \end{pmatrix}, \quad (14)$$

or

$$\kappa_{ij} = -\theta_{i,j}^c.$$

Finite Element Formulation

Nodal and Internal Variables

In the FEM formulation of a Cosserat continuum, each node, N , is associated with three displacement and three rotational degrees of freedom. The vector of nodal degrees of freedom is defined as:

$$\bar{\mathbf{U}} = [\bar{\mathbf{u}} \quad \bar{\boldsymbol{\theta}}] = [\bar{u}_1 \quad \bar{u}_2 \quad \bar{u}_3 \quad \bar{\theta}_1 \quad \bar{\theta}_2 \quad \bar{\theta}_3]. \quad (15)$$

Using a notation similar to Voigt notation, the second-order strain and curvature tensors can be expressed in the following vectorial form:

$$\begin{aligned} \boldsymbol{\gamma} &= [\gamma_{11} \quad \gamma_{22} \quad \gamma_{33} \quad \gamma_{23} \quad \gamma_{32} \quad \gamma_{13} \quad \gamma_{31} \quad \gamma_{12} \quad \gamma_{21}], \\ \boldsymbol{\kappa} &= [\kappa_{11} \quad \kappa_{22} \quad \kappa_{33} \quad \kappa_{23} \quad \kappa_{32} \quad \kappa_{13} \quad \kappa_{31} \quad \kappa_{12} \quad \kappa_{21}]. \end{aligned} \quad (16)$$

Finally, using FEM discretization techniques and the interpolation function, ϕ , the strain and curvature field can be interpolated, with respect to the vector of nodal degrees of freedom, $\bar{\mathbf{u}}$ and $\bar{\boldsymbol{\theta}}$, through:

$$\begin{bmatrix} \boldsymbol{\gamma} \\ \boldsymbol{\kappa} \end{bmatrix} = \mathbf{B}_N \begin{bmatrix} \bar{\mathbf{u}}_N \\ \bar{\boldsymbol{\theta}}_N \end{bmatrix}. \quad (17)$$

The operator, \mathbf{B}_N , has a block structure and is expressed in the following form:

$$\mathbf{B}_N = \begin{pmatrix} \mathbf{B}_{N1} & \mathbf{B}_{N2} \\ [\mathbf{0}]_{9 \times 3} & \mathbf{B}_{N3} \end{pmatrix}, \quad (18)$$

with:

$$\begin{aligned} \mathbf{B}_{N1} &= \begin{pmatrix} \phi_{N,1} & 0 & 0 & 0 & 0 & 0 \\ 0 & \phi_{N,2} & 0 & 0 & \phi_{N,3} & 0 \\ 0 & 0 & \phi_{N,3} & \phi_{N,2} & 0 & \phi_{N,1} \\ & \phi_{N,3} & 0 & \phi_{N,2} & & \\ & 0 & \phi_{N,1} & 0 & & \\ & 0 & 0 & 0 & & \end{pmatrix}^T, \\ \mathbf{B}_{N2} &= \begin{pmatrix} 0 & 0 & 0 & -\phi_N & \phi_N & 0 & 0 & 0 & 0 \\ 0 & 0 & 0 & 0 & \phi_N & -\phi_N & 0 & 0 & 0 \\ 0 & 0 & 0 & 0 & 0 & 0 & -\phi_N & \phi_N & 0 \end{pmatrix}^T, \\ \mathbf{B}_{N3} &= - \begin{pmatrix} \phi_{N,1} & 0 & 0 & 0 & 0 \\ 0 & \phi_{N,2} & 0 & \phi_{N,3} & 0 \\ 0 & 0 & \phi_{N,3} & 0 & \phi_{N,2} \\ & \phi_{N,3} & 0 & \phi_{N,2} & 0 \\ & 0 & 0 & \phi_{N,1} & \\ & 0 & \phi_{N,1} & 0 & 0 \end{pmatrix}^T, \end{aligned} \quad (19)$$

where ϕ_N is the shape function for the N th node and is used for interpolation of both the displacement field and the rotation field.

Material Stiffness Matrix

The material stiffness matrix is expressed in the following form:

$$\mathbf{K}_{NM}^{\text{mat}} = \mathbf{B}_N^T \mathbf{D} \mathbf{B}_M, \quad (20)$$

where \mathbf{B} is defined by Equations 17 and 18, and \mathbf{D} is a block diagonal matrix, which relates the stress and couple stress measures to their work conjugate measures, strains and curvatures, respectively, through the appropriate constitutive law, $\mathbf{D} = [\mathbf{D}_1, \mathbf{D}_2]$.

CONSTITUTIVE EQUATIONS

The Cosserat formulation provides an enhanced mathematical description of the mechanics of a deformable body through the introduction of higher-order kinematic and kinetic variables. The appealing aspect of the Cosserat theory is that a physically meaningful link can be made between the kinetic and kinematic variables of the Cosserat theory and the behavior of some materials with microstructure, such as granular, blocky or layered materials. The additional Cosserat parameters for each material should be determined based on the mechanical response of the particular microstructure. Constitutive equations for the 2-D behavior of particulate layered and blocky [14,15,20,21] materials have been widely discussed in the past. Recently, the following constitutive relations were proposed for the 3-D analysis of layered materials [27,28]:

$$\widehat{\mathbf{D}}_1 = \begin{bmatrix} \mathbf{A}_n & [\mathbf{0}]_{3 \times 6} \\ [\mathbf{0}]_{6 \times 3} & \mathbf{A}_G \end{bmatrix}, \quad (21)$$

and:

$$\widehat{\mathbf{D}}_2 = \begin{bmatrix} \begin{bmatrix} [(1-\nu)B & 0 \\ 0 & (1-\nu)B] & [\mathbf{0}]_{2 \times 5} \\ & [\mathbf{0}]_{5 \times 2} & [\mathbf{0}]_{5 \times 5} \end{bmatrix} & [\mathbf{0}]_{7 \times 2} \\ & [\mathbf{0}]_{2 \times 7} & \begin{bmatrix} B & \nu B \\ \nu B & B \end{bmatrix} \end{bmatrix}, \quad (22)$$

where:

$$\begin{aligned} A_{11} &= A_{22} = \frac{E}{1 - \nu^2 - \frac{\nu^2(1+\nu)^2}{(1-\nu^2+E/hk_n)}}, \\ A_{33} &= \frac{(1-\nu)E}{(1+\nu)(1-2\nu) - \frac{(1-\nu)E}{(E/hk_n)}}, \\ A_{12} &= A_{21} = \frac{\nu E}{(1+\nu)(1-2\nu) + (1-\nu)E/hk_n}, \end{aligned}$$

$$\begin{aligned}
A_{13} &= A_{31} = A_{23} = A_{32} \\
&= \frac{E\nu(E + hk_n(1 - \nu))}{(1 - \nu)(2hk_n\nu^2 - (1 + \nu)(E + hk_n))}, \\
G_{11} &= \frac{Ghk_s}{G + hk_s}, G_{22} = G + G_{11},
\end{aligned} \tag{23}$$

and:

$$B = \frac{Eh^2}{12(1 - \nu^2)} \left(\frac{G - G_{11}}{G + G_{11}} \right). \tag{24}$$

In the above expressions, E , G and ν correspond to the Young's modulus, shear modulus, and Poisson ratio, respectively, of the intact material comprising the layers, h is the layer thickness, and k_n and k_s are the normal and shear stiffness of the layer interface, with units N.m^{-1} . The $\hat{\cdot}$ sign indicates that the constitutive equations are expressed in the local coordinates of the layers.

It is emphasized that the constitutive equations of a Cosserat material are expressed for a representative elementary volume that encompasses a sequence of microstructures (see Figure 2a), by applying an equivalent continuum concept [36,37]. The characteristic volume of a Cosserat continuum is, therefore, fundamentally different in its assumption and behavior from the characteristic volume of a classical continuum, which is assumed to be homogenous, i.e. free of gaps, voids and discontinuities. For more details on the derivation of the above equations refer to Appendix A.

Finally, it should be noted that the above constitutive equations are based on the mechanical considerations of a plate component [34]. In order to use the above relations, it is necessary to change the sign of the first column of \mathbf{B}_{N3} in Equation 19 to be consistent with plate theory [34].

GOVERNING EQUATIONS AND FORMULATION OF INTERFACE ELEMENTS

Interface or joint elements are devised to take into account the sliding and separation that may occur along the discontinuity surface between adjacent blocks. Based on assumptions regarding their behavior, numerous formulations for interface elements have been proposed [38]. The potential function or virtual work for this element are obtained from the linear momentum equation by assuming an infinitesimal thickness for the joint element, and by disregarding the kinetic (stress) and kinematic (strain) terms that are associated with the thickness (y direction). The internal potential energy, Π^{int} , or the virtual work, δW^{int} , associated with deformation at the interface are expressed as:

$$\Pi^{\text{int}} = \frac{1}{2} \int_A \varepsilon_{ij} \sigma_{ij},$$

or:

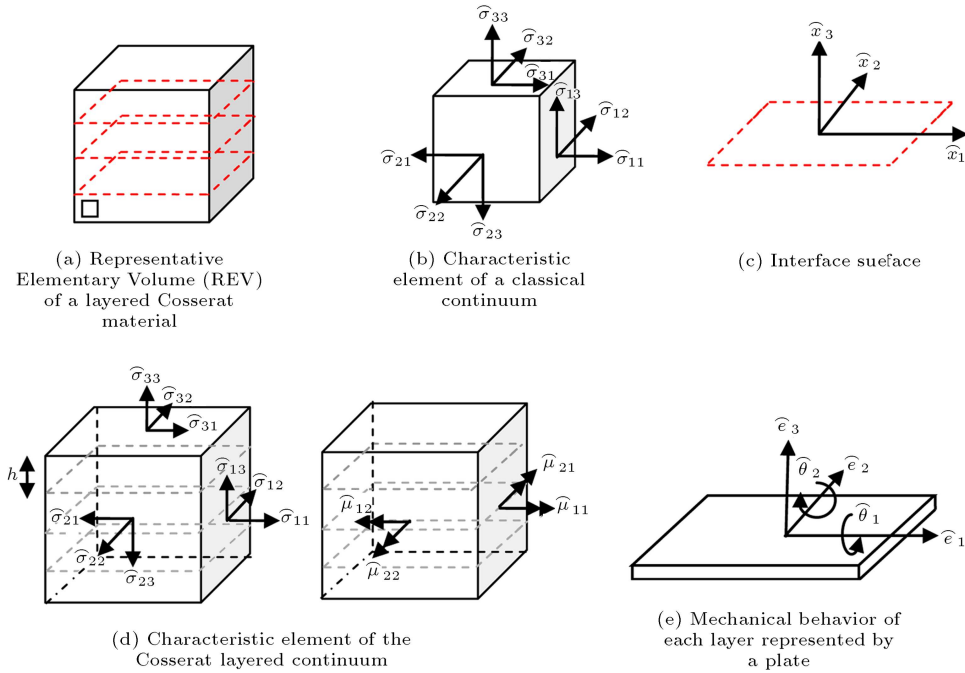


Figure 2. (a) Representative elementary volume of a layered material; (b) Characteristic volume of a homogeneous classical continuum; (c) Interface between layers; (d) Characteristic volume of a Cosserat layered continuum and the non-zero stress and couple-stress components acting on it; (e) 3-D representation of mechanics of a single plate.

$$\delta W^{\text{int}} = \int_A \delta \varepsilon_{ij} \sigma_{ij}. \quad (25)$$

Assuming infinitesimal thickness for the interface gives rise to three kinematic variables in 3-D that can be expressed in terms of sliding displacements in the direction of the two local axes of the interface surface and normal displacement in the direction perpendicular to the surface of the element. For example, in a 2-D (line) element (see Figure 3), the potential function reduces to:

$$\begin{aligned} \Pi = & \frac{1}{2} \left[\int_{-l/2}^{+l/2} k_n (\nu_{\text{top}} - \nu_{\text{bottom}})^2 dx \right. \\ & \left. + \int_{-l/2}^{+l/2} k_s (u_{\text{top}} - u_{\text{bottom}})^2 dx \right], \end{aligned} \quad (26)$$

or:

$$\Pi = \frac{1}{2} \int_A \mathbf{u}^T \mathbf{K} \mathbf{u} dA - \int_{\Gamma} \mathbf{u}^T \mathbf{F} d\Gamma,$$

where k_n and k_s are the normal and shear stiffness at the contact with units N.m^{-1} , \mathbf{u} is the displacement vector, \mathbf{K} is the stiffness matrix, and \mathbf{F} is the internal force vector for the joint element, derived from minimization of potential energy:

$$\frac{\partial \Pi}{\partial \mathbf{u}} = \int_{-l/2}^{+l/2} \mathbf{K} \mathbf{u} dx - \int_{\Gamma} \mathbf{F} d\Gamma = 0, \quad (27)$$

where:

$$K_{ij} = \frac{\partial \Pi}{\partial u_i \partial u_j}, \quad F_i = \frac{\partial \Pi}{\partial u_i}. \quad (28)$$

In finite element models that utilize interface elements, the stiffness and force terms arising from Equation 28 are assembled to the global system of equations that incorporate the stiffness and force terms of regular continuum elements representing the intact materials.

NUMERICAL EXAMPLES

Cantilever Layered Strip Plate Subjected to a Transverse Shear Force

This example concerns a layered strip plate subjected to a 1 MPa transverse shear traction applied to the



Figure 3. Geometry of an interface element; interface can be assumed to be with or without filling materials.

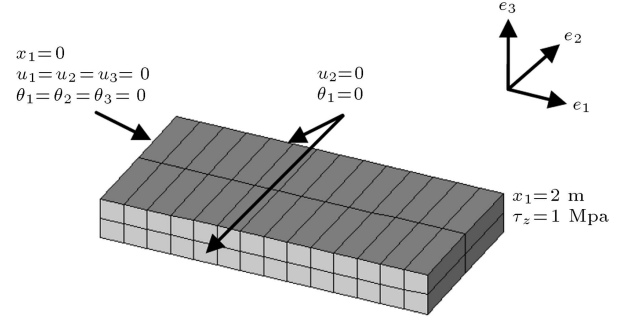


Figure 4. Geometry and boundary conditions for the layered strip plate.

end of the plate. The geometry, boundary conditions and FEM discretization are shown in Figure 4. The plate has a length of 2 m, a height of 0.25 m and is divided into four horizontal layers independent of the number of elements used along the thickness. Each layer has a thickness of 0.0625 m. The shear stiffness of the interface, k_s , varies from zero to a very large value ($1e15 \text{ MPa/m}$). Due to the boundary conditions in the x_2 direction, the plate behaves as an extruded beam.

Figures 5 to 7 show the distribution of shear stresses and micromoments occurring in the layered strip plate. In the Cosserat formulation, the internal length parameter of the material (the layer thickness) is considered in the formulation. In this example, the layer bending mechanism sustains the shear load applied to the system. In the case where k_s is zero, the shear stress through the depth of the beam, i.e. σ_{31} , remains zero, while the shear stress along the thickness

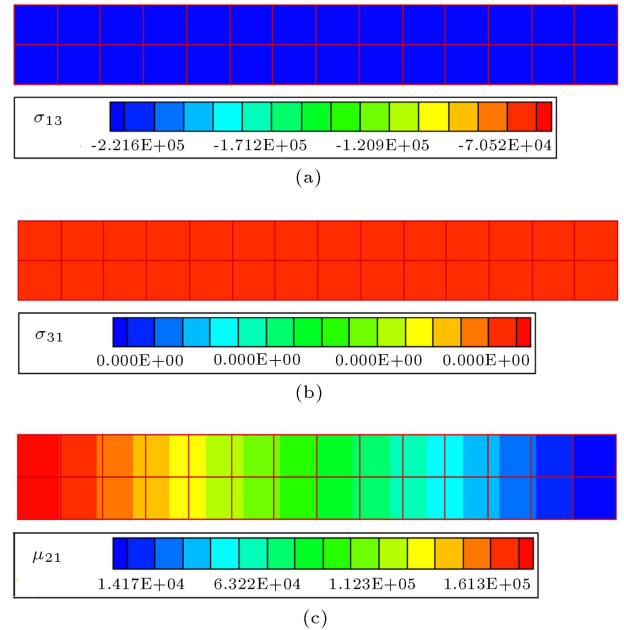


Figure 5. Distribution of shear stress σ_{13} , σ_{31} and micromoment μ_{21} in a layered strip plate ($k_s = 0$, $\tau = 10 \text{ KPa}$).

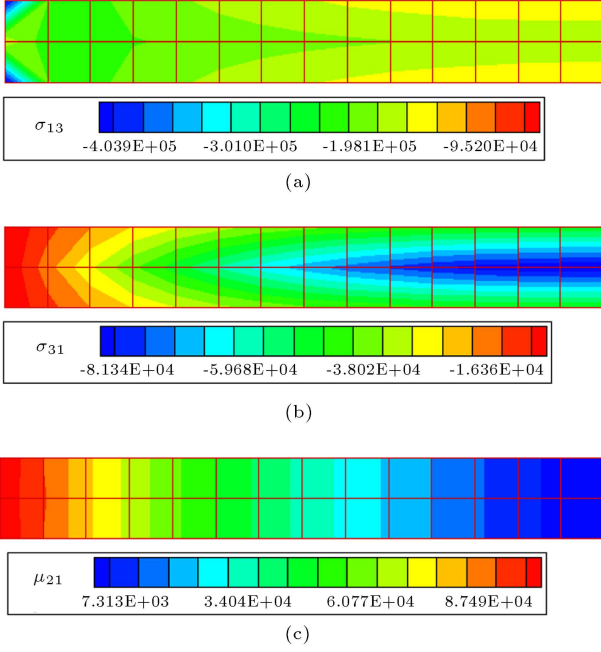


Figure 6. Distribution of shear stress σ_{13} , σ_{31} and micromoment μ_{21} in a layered strip plate ($k_s = 100$ MPa/m, $\tau = 10$ KPa).

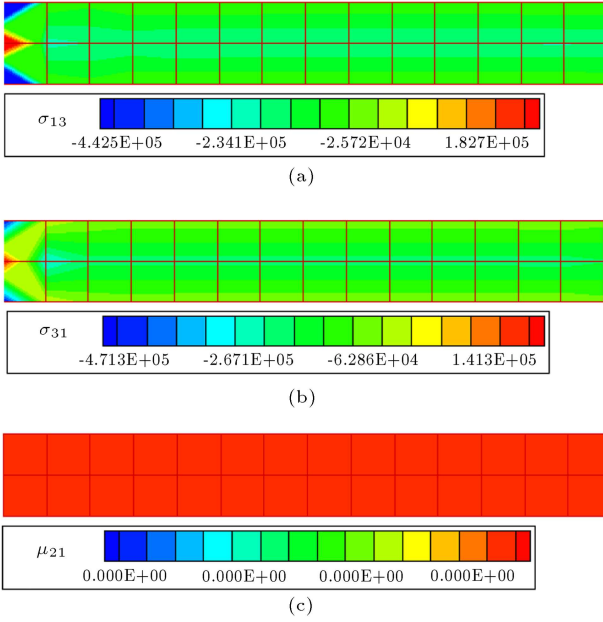


Figure 7. Distribution of shear stress components σ_{13} , σ_{31} and micromoment μ_{21} in a layered strip plate ($k_s = \infty$, $\tau = 10$ KPa).

of the beam, i.e. σ_{13} , develops proportional to the magnitude of the applied force. As k_s increases, the difference in the conjugate components of shear stresses reduces and, in the case where $k_s \rightarrow \infty$, the shear stresses become symmetric. In each case, the difference between the conjugate shear stress components is

equilibrated by the gradient of the micromoment along the axis of the beam.

Figure 8 shows the vertical displacement at the tip of the beam vs. $\log(k_s)$. Over the entire range of k_s , the results were compared to the results predicted by the FEM explicit joint model using the Phase² FEM package [39]. For the case where the shear stiffness of the joints is equal to zero, the extruded beam reduces to 4 non-interacting beams, while for very large values of k_s , the model reduces to a homogeneous thick beam with a depth of 0.25 m. For these two limit cases, where $k_s \rightarrow 0$ and $k_s \rightarrow \infty$, the solution is compared to the analytical solution for the deflection of a beam [40]:

$$u_3(l) = \frac{4\tau_s l^3}{Eh^2}(1 - \nu^2). \quad (29)$$

It should be noted that in the Cosserat solution, layer thickness is an input parameter for the material. Therefore, depending on the geometry of a given structure, partial layers may develop, which may not be physically meaningful.

Column of Jointed Material Subjected to a Uniaxial Compressive Traction on Top

This example concerns a layered column with a width of 1 m and a height of 2 m (Figure 9). Both horizontal and vertical displacements are fixed at the bottom of the sample. In the Cosserat model, the Cosserat rotational degrees of freedom are also constrained at the bottom. A constant uniform traction of 5 MPa is applied at the top of the column. The intact rock is assumed to be isotropic with a Young's modulus of 10 GPa and a Poisson ratio of 0.25.

In order to compare the finite element Cosserat solution with the explicit joint model, four different

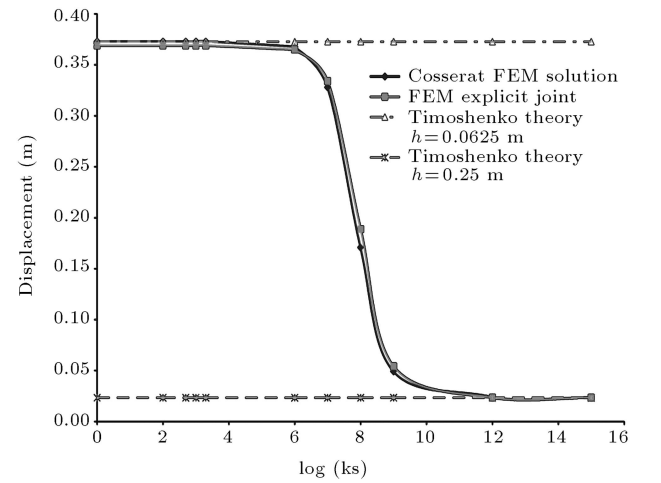


Figure 8. Effect of the interaction of the layers on the vertical displacement of the layered strip plate ($h = 0.0625$ m, $\tau = 200$ KPa).

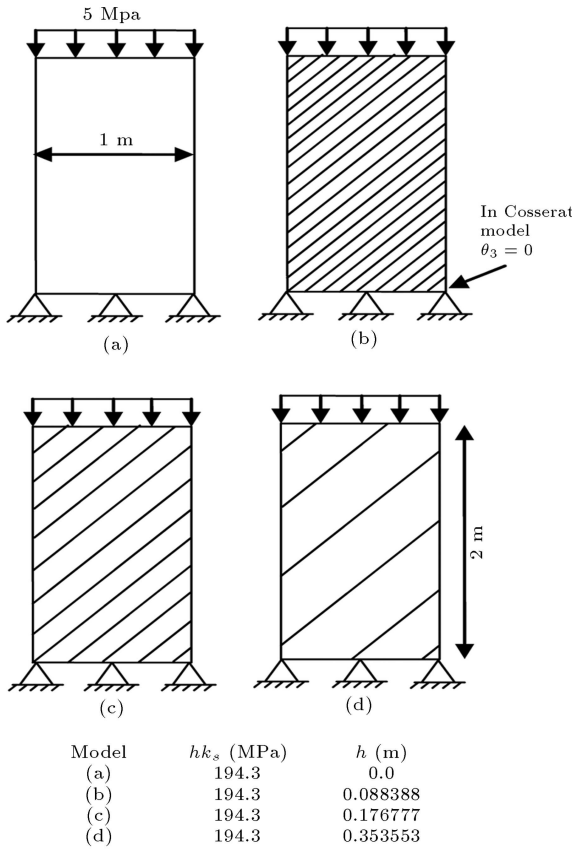


Figure 9. Boundary conditions and joint spacing of the column of layered rock subjected to a uniform axial pressure.

problems, with a constant equivalent shear modulus but varying values of h , are considered. The equivalent shear modulus is obtained from $G_{eq} = (1/G + 1/hk_s)^{-1}$. In all samples, the product of hk_s used in relations of Equation 23 was constant and equal to 194 MPa, but different values of h and k_s were assigned to the layer thickness and interface shear stiffness, respectively. In all cases, a relatively large value is chosen for hk_n . Thus, in the local coordinates of the layers, $\hat{E}_{11} = \hat{E}_{22}$.

Figure 9a shows a case in which the joint spacing is so close that the effect of layer thickness (bending rigidity) is insignificant. Therefore, instead of utilizing interface elements, a conventional anisotropic material with a shear modulus of G_{eq} is used for the analysis. In the Cosserat solution, this case was solved by assigning a zero value to B , while hks was constant and equal to 194 MPa.

Figures 9b to 9d show the geometry and joint spacing used for the finite element explicit interface solution. In the explicit interface models, layers are simulated using joint (interface) elements with the value of k_s assigned to joints, shown in Figure 9. In the equivalent Cosserat model of Figures 9b to 9d, joints are not explicitly defined, but values of h and k_s are defined as material input parameters,

and are introduced into the formulation through the constitutive rotations of Equations 22 to 24.

Figure 10 shows the values of the maximum displacement of the column predicted by the FEM Cosserat solution and the FEM explicit joint model. It is emphasized that for model 9a in the Cosserat formulation, the value of bending stiffness (Equation 24) is set to zero and, in the classical FEM formulation, instead of using explicit interface elements, a transversely isotropic material is used.

From Figure 10, it is clear that the Cosserat formulation is as accurate as the explicit interface model in predicting the deformation response of this problem.

Figures 11 and 12 demonstrate the effect of layer thickness on the pattern of deformation of the layered sample predicted by the Cosserat solution and the FEM explicit joint solution, respectively. Figures 11 and 12 indicate that the Cosserat model can correctly capture the effect of layer thickness, and therefore predicts a similar displacement field, compared to the explicit interface model. The deformed shapes also show the smeared nature of the Cosserat solution. In other words, the jumps or discontinuities that are present in results captured by the explicit interface model are not present in the Cosserat solution, which predicts a continuous displacement field. However, the results are consistent, in terms of both the values and the pattern of the displacements.

Finally, by using the Cosserat formulation with a zero value of bending coefficient, it is shown that the classical theory of transversely isotropic materials is a limit case of the Cosserat theory of layered materials, in which the bending stiffness of the layers is disregarded.

Circular Excavation in Layered Media with in-Plane Layers

In this example, the elastic response of a series of underground excavations in layered rock is studied

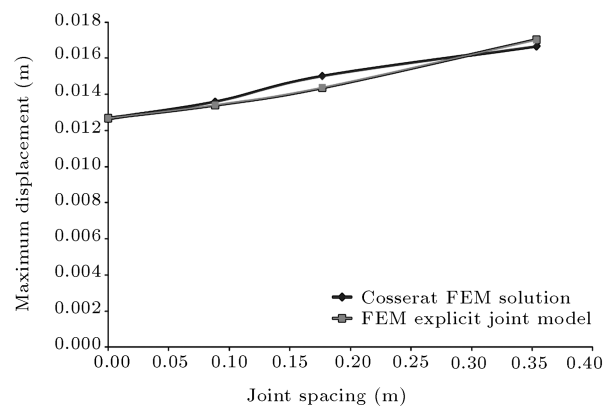


Figure 10. Maximum displacements of the jointed column vs. layer thickness.

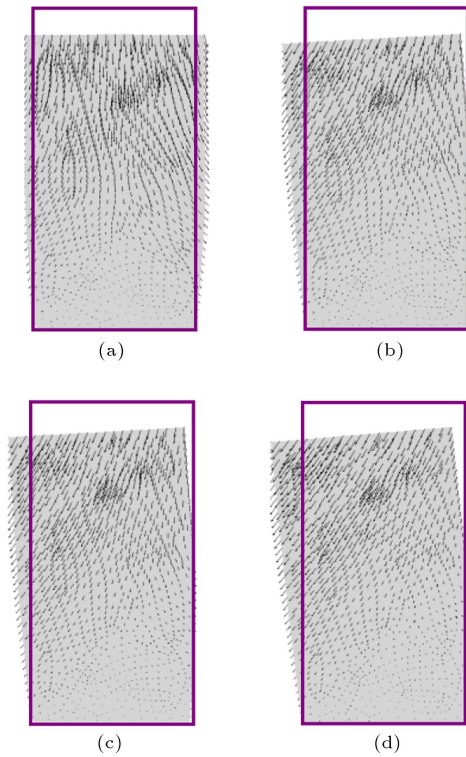


Figure 11. Total displacement predicted by the Cosserat model for a column of layered rock subjected to a uniform axial pressure. (a) $h = 0$; (b) 0.088; (c) 0.177; (d) 0.354 m.

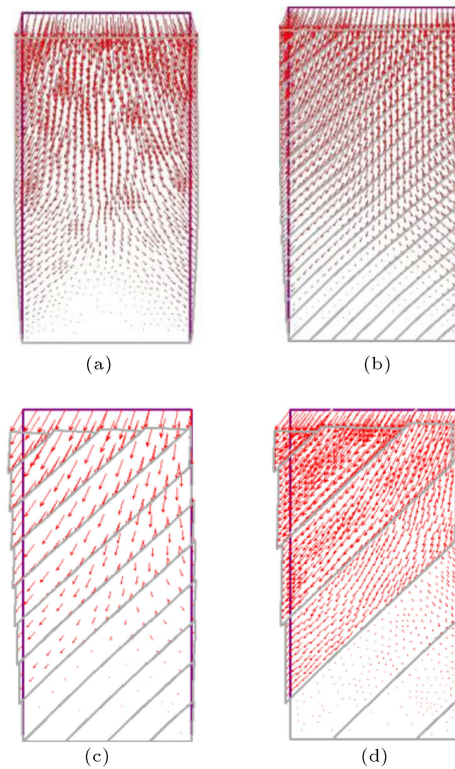


Figure 12. Total displacement predicted by the explicit joint model for a column of layered rock subjected to a uniform axial pressure. (a) $h = 0$; (b) 0.088; (c) 0.177; (d) 0.354 m.

using the FEM Cosserat solution and the FEM explicit interface model. This example shows that the FEM Cosserat solution can confidently be applied to large scale engineering problems as an alternative to the FEM explicit interface model.

The geometry, boundary conditions and mesh discretization of the FEM Cosserat solution are shown in Figure 13. The joint orientations and information regarding the mesh discretization of the Phase² explicit joint model are presented in Figure 14. The top boundary is subjected to a uniform pressure with a magnitude of 100 MPa, while all other boundaries are fixed. In order to compare the results to Phase², (which is a 2-D application code), in the 3-D Cosserat model, the displacements associated with the out-of-plane direction, u_y , and the Cosserat rotation around the x axis, θ_x , are constrained. As a result, the full 3-D model behaves similarly to a 2-D plane strain problem, and it is justified to use one element in the out-of-plane direction.

The intact rock is modeled as an isotropic elastic material with a Young's modulus of 17.8 GPa and a Poisson ratio of 0.25. The joints are spaced 2.5 m apart. The elastic response of the model is investigated for two cases:

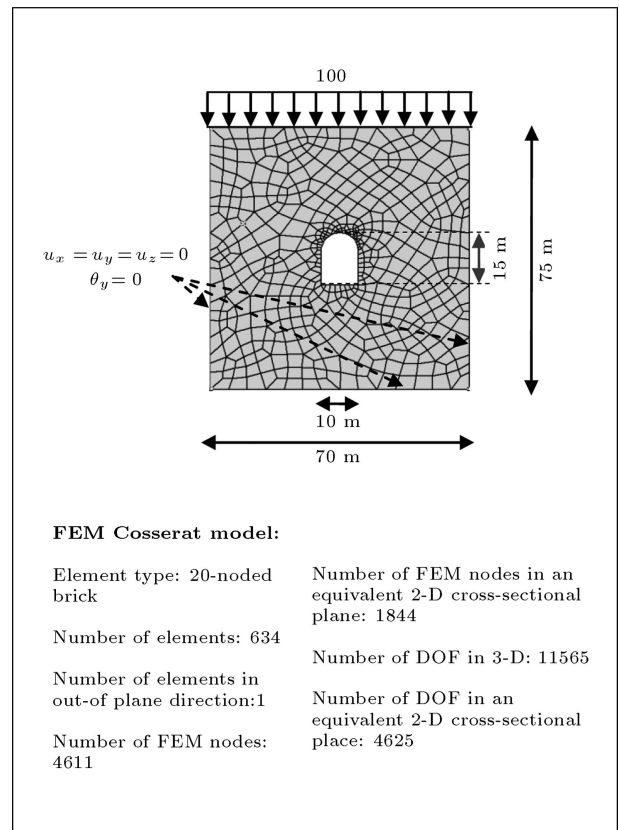


Figure 13. Geometry, mesh discretization, and boundary conditions for the FEM Cosserat solution of a 2-D-extruded tunnel excavated in layered rock.

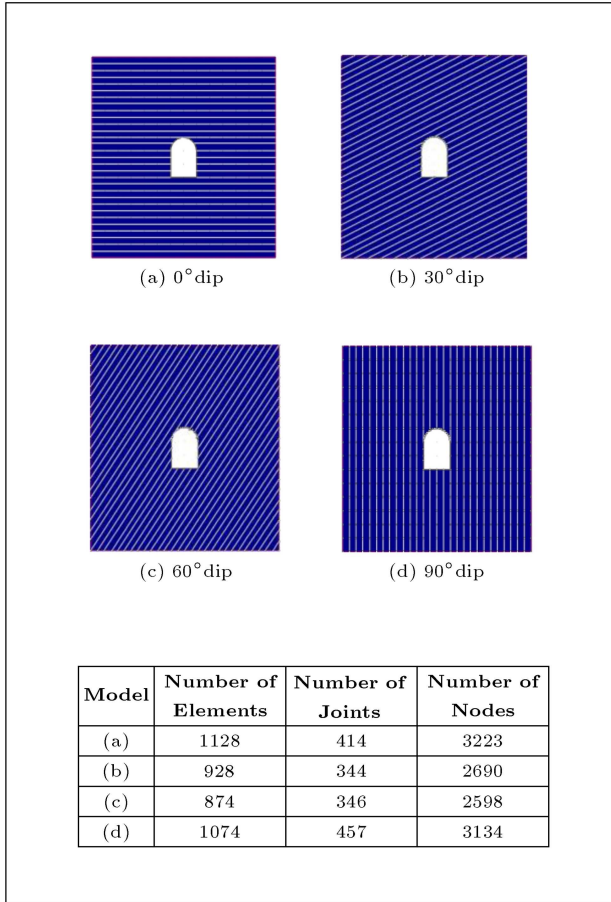


Figure 14. Geometry, mesh specifications, and joint orientations for the FEM explicit joint model of a 2-D-extruded tunnel excavated in layered rock.

- i) $k_n = 20$ GPa/m and $k_s = 200$ MPa/m,
- ii) $k_n/E = 1e10$ and $k_s = 200$ MPa/m.

The Cosserat solution is compared to the Phase² explicit joint model for values of $B > 0$, and to the classical transversely isotropic model for the case where $B = 0$. The latter is a limit case of the Cosserat model in which joint spacing is small compared to the external dimensions of the problem, and therefore the bending rigidity of layers can be disregarded.

Figure 15 shows values of the total elastic displacement at the center of the tunnel roof for case (i). In this case, all models predict similar values for the total displacement at the top of the tunnel. Figure 16 shows values of the total elastic displacement at the center of the tunnel roof for case (ii). In case (ii), k_n is relatively large. Therefore, the effect of the bending stiffness of the layers can be observed in the results. Due to the bending mechanism that resists the load, the displacements of the model with horizontal layers are approximately 20% less than cases where joints are oriented vertically. However, the classical transversely isotropic model yields similar results for both cases

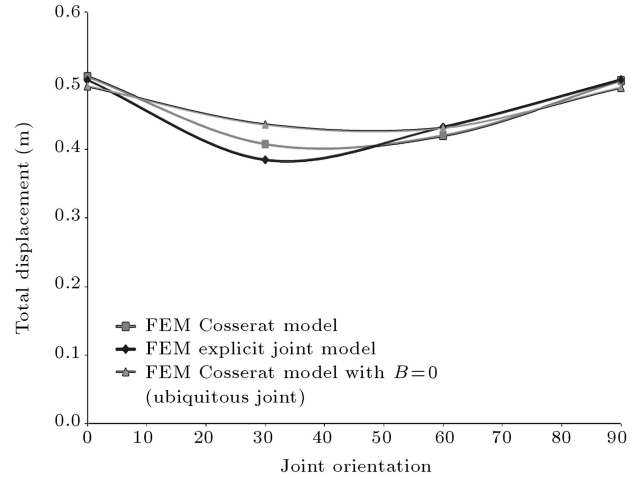


Figure 15. Total elastic displacement at the center of the tunnel roof for joints with $k_n = 20000$ MPa/m and $k_s = 200$ MPa/m.

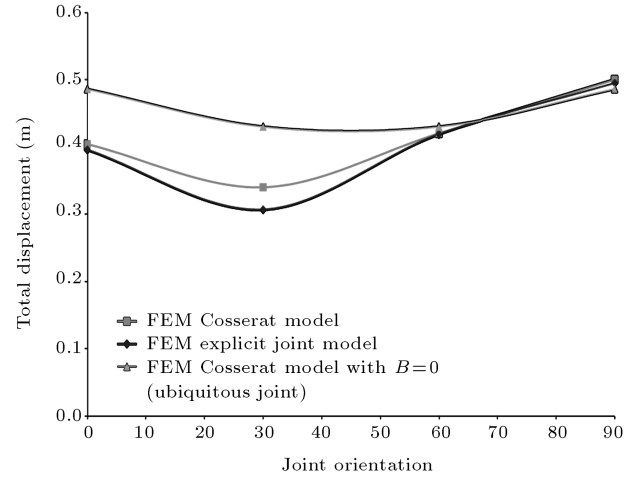


Figure 16. Total elastic displacement at the center of the tunnel roof for joints with $k_n/E = 1e10$ and $k_s = 200$ MPa/m.

(provided that the ratio of k_n/E is relatively large), since the shear modulus of the equivalent material is equal in the conjugate directions. It is clear that by disregarding the bending rigidity of the layers, the FEM solution, using a transversely isotropic material, can significantly overestimate the elastic displacements.

The induced anisotropy influenced the magnitude and location of the maximum displacement on the boundary of the excavation. Figures 17 and 18 show the contours of the total displacement predicted by the FEM Cosserat model and the explicit joint model for two different layer orientations.

It is clear that by using a relatively coarse mesh that is totally independent of layer orientation and layer spacing, the finite element Cosserat model predicts the displacement response of these examples within a good accuracy, compared to the finite element model, which utilizes explicit interface elements.

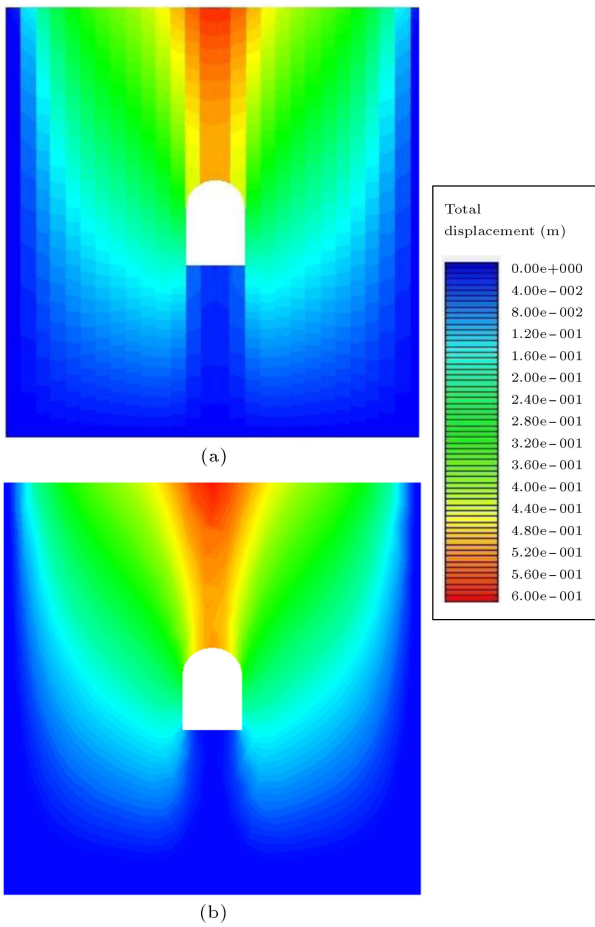


Figure 17. Contours of total elastic displacement predicted by (a) FEM explicit joint model and (b) FEM Cosserat model for joints oriented vertically.

CONCLUSION

This paper focuses on a comparison of the finite element Cosserat solution and the finite element solution, which applies an interface technology to the analysis of layered media. The fundamental assumption, formulation and solution of both approaches are investigated and compared.

It is discussed that in the Cosserat theory, the effect of reduced shear and normal properties at the interface and the existing microstructure of the material, or layer thickness, are all incorporated into the constitutive equations. The reduced shear and normal properties at the interface are reflected in the elastic coefficients that relate stress to its work conjugate strain measure, while the layer thickness is reflected in the constitutive relations that relate Cosserat micromoments to their work conjugate pair, i.e. curvatures.

In the FEM solution, based on a classical continuum theory, interfaces between the layers are explicitly simulated by utilizing specially devised elements that relax the continuity assumption at an infinitely thin

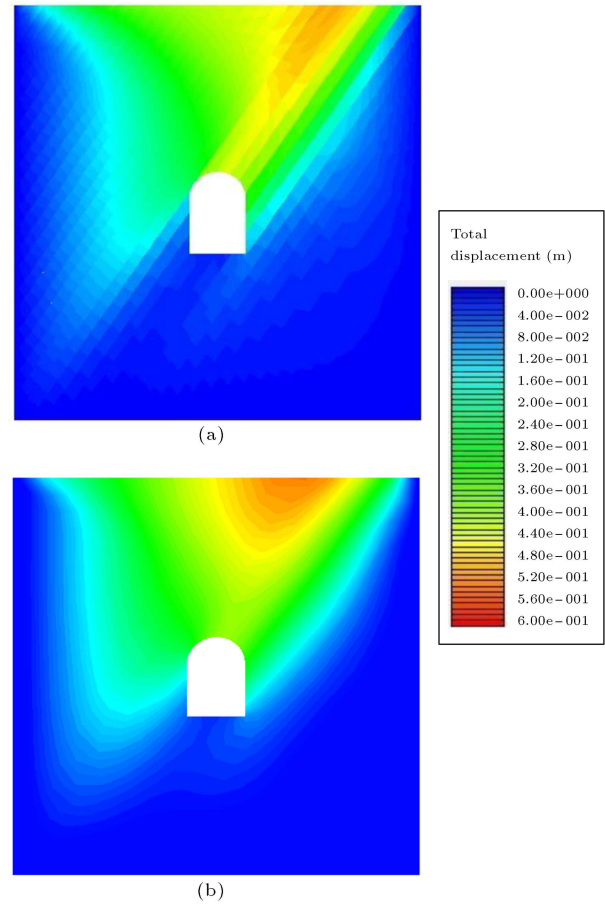


Figure 18. Contours of total elastic displacement predicted by (a) FEM explicit joint model and (b) FEM Cosserat model for joints oriented at 60° with respect to a horizontal plane.

surface between two layers. The effect of properties of interfaces is incorporated into the constitutive equations of joint (interface) elements, and due to the explicit simulation of layers, the effect of layer thickness is naturally captured in the model.

In this paper, the deformed shape and displacement field predicted by the aforementioned solutions are compared in a number of benchmark examples with various boundary conditions, interaction conditions between the layers, layer thicknesses and layer orientations. It was shown that the FEM Cosserat formulation demonstrates a high level of consistency with models that explicitly simulate the interfaces.

From a computational aspect, the degree of complexity of the solution depends on the total degrees of freedom of the problem. If layers are to be modeled explicitly, the analysis of highly jointed media becomes impractical, except for small scale problems. The Cosserat formulation provides a suitable technique for such analysis, since the internal length is implicit in the governing equations of the system, and the FEM mesh is independent of the orientation and spacing of the joints.

REFERENCES

1. Cosserat, E. and Cosserat F., *Théorie des Corps Deformable*, Hermann, Paris (1909).
2. Voigt, W. "Theoretische studien über die elasticitätsverhältnisse der krystalle (Eng. translation of title: Theoretical Studies of the Elastic Behavior of Crystals)", *Abhandlungen Gesellschaft Wissenschaften Göttingen*, p. 34 (1887).
3. Kroner, E. "Mechanics of generalized continua. Proc.", *IUTAM Symposium Generalized Cosserat Continuum and Continuous Theory of Dislocations with Applications*, Springer-Verlag, Berlin (1967).
4. Mindlin, R.D. "Second gradient of strain and surface-tension in linear elasticity", *Int. J. Solids Struct.*, **1**(4), pp. 417-438 (1965).
5. Shaefer, H. "Das Cosserat-kontinuum", *ZAMM J. Appl. Math. Mech. / Z. Angew. Math. Mech.*, **47**, pp. 485-498 (1967).
6. Naghdi, P.M. "The theory of plates and shells", in *S. Flugge Handbuch der Physics*, C. Truesdell, Ed. Springer-Verlag, Berlin, pp. 425-640 (1972).
7. Naghdi, P.M. "Finite deformation of elastic rods and shells", *Proceeding of the IUTAM Symposium Finite Elasticity*, Bethlehem, Pennsylvania, pp. 17-103 (1982).
8. Green, A.E., Naghdi, P.M. and Wenner, M.L., *On the Theory of Rods, I. Derivation from the Three-Dimensional Equations*, Royal Society of London, A337, pp. 451-483 (1974).
9. Green, A.E., Naghdi, P.M. and Wenner, M.L., *On the Theory of Rods, II. Developments by Direct Approach*, Royal Society of London, A337, pp. 485-507 (1974).
10. Rubin, M.B. "Cosserat theories: shells, rods and points", *Solid Mechanics and its Applications*, **79**, Kluwer, The Netherlands (2000).
11. Nadler, B. and Rubin, M.B. "A new 3-D finite element for nonlinear elasticity using the theory of a Cosserat point", *Int. J. Solids Struct.*, **40**, pp. 4585-4614 (2003).
12. Nadler, B. and Rubin, M.B. "Determination of hour-glass coefficients in the theory of a Cosserat point for nonlinear elastic beams", *Int. J. Solids Struct.*, **40**, pp. 6163-6188 (2003).
13. Naghdi, P.M. and Rubin, M.B. "Constrained theories of rods", *J. Elasticity*, **14**, pp. 343-361 (1984).
14. Mühlhaus, H.B. "Scherfugenanalyse bei Granularem Material im Rahmen der Cosserat Theorie", *Ingenieur Archiv.*, **56**, pp. 389-399 (1986).
15. Mühlhaus, H.B. and Vardoulakis, I. "The thickness of shear bands in granular materials", *Geotechnique*, **37**(3), pp. 271-283 (1987).
16. de Borst, R. and Mühlhaus, H.B. "Gradient-dependent plasticity - formulation and algorithmic aspects", *Int. J. Numer. Meth. Eng.*, **35**(3), pp. 521-539 (1992).
17. de Borst, R. "A generalization of J2-flow theory for polar continua", *Comput. Meth. Appl. Mech. Eng.*, **103**(3), pp. 347-362 (1993).
18. Froio, F., Tomassetti, G. and Vardoulakis, I. "Mechanics of granular materials: The discrete and the continuum descriptions juxtaposed", *Int. J. Solids Struct.*, **43**, pp. 7684-7720 (2006).
19. Arslan, H. and Sture, S. "Evaluation of a physical length scale for granular materials", *Comp. Mat. Sci.*, **42**, pp. 525-530 (2008).
20. Mühlhaus, H.B. "Continuum models for layered and blocky materials", *Comprehensive Rock Mechanics*, Pergamon Press, Oxford (1993).
21. Mühlhaus, H.B. "A relative gradient method for laminated materials", *Continuum Models for Materials with Microstructure*, Wiley, Toronto (1995).
22. Adhikary, D.P. and Dyskin, A.V. "A Cosserat continuum for layered materials", *Comput. Geotech.*, **20**(1), pp. 15-45 (1997).
23. Adhikary, D.P. and Dyskin, A.V. "Modelling of progressive and instantaneous failures of foliated rock slopes", *Rock Mech. Rock Eng.*, **40**(4), pp. 349-362 (2007).
24. Adhikary, D.P. and Guo, H. "An orthotropic Cosserat elasto-plastic model for layered rocks", *Rock Mech. Rock Eng.*, **35**(3), pp. 161-170 (2002).
25. Adhikary, D.P., Mühlhaus, H.B. and Dyskin, A.V. "Modelling the large deformations in stratified media; the Cosserat continuum approach", *Mech. Cohesive-Frictional Mat.*, **224**(3), pp. 195-213 (1999).
26. Adhikary, D.P., Mühlhaus, H.B. and Dyskin, A.V. "A numerical study of flexural buckling of foliated rock slopes", *Int. J. Numer. Anal. Meth. Geomech.*, **25**, pp. 871-884 (2001).
27. Riahi, A. "3-D finite element Cosserat continuum simulation of layered geomaterials", PhD Thesis, University of Toronto, Toronto (2008).
28. Riahi, A. and Curran, J.H. "Full 3-D finite element Cosserat formulation with application in layered structures", *Appl. Math. Model.*, **33**, pp. 3450-3464 (2009).
29. Riahi, A., Curran, J.H. and Bidhendi, H. "Buckling analysis of 3-D layered structures using a Cosserat continuum approach", *Comput. Geotech.*, **36**, pp. 1101-1112 (2009).
30. Dai, C., Mühlhaus, H.B., Meek, J. and Duncan, M. "Modeling of blocky rock masses using the Cosserat method", *Int. J. Rock Mech. Min. Sci. Geomech. Abstr.*, **33**(4), pp. 425-432 (1996).
31. Sulem, J. and Mühlhaus, H.B. "A continuum model for periodic two-dimensional block structures", *Mech. Cohesive-Frictional Mat.*, **2**, pp. 31-46 (1997).
32. Stefanou, I., Sulem, J. and Vardoulakis, I. "Three-dimensional Cosserat homogenization of masonry structures: elasticity", *Acta. Geotechnica*, **3**, pp. 71-83 (2008).
33. Truesdell, C. and Toupin, R. "The classical field theories", *Handbuch der Physik*, **3**(1), Edited by Flugge, Springer-Verlag, Berlin, pp. 226-793 (1960).

34. Szilard, R., *Theories and Applications of Plate Analysis: Classical, Numerical, and Engineering Methods*, Hoboken, John Wiley (2004).
35. Steinmann, P. "A micropolar theory of finite deformation and finite rotation multiplicative elastoplasticity", *Int. J. Solids Struct.*, **1**(8), pp. 1063-1084 (1994).
36. Sharma, K.G. and Pande, G.N. "Stability of rock masses reinforced by passive, fully-grouted rock bolts", *Int. J. Rock Mech. Min. Sci. Geomech. Abstr.*, **25**(5), pp. 273-285 (1988).
37. Zvolinski, N.V. and Shkhinek, K.N. "Continuum model for a laminar elastic medium", *Solid Mechanics*, **19**(1), pp. 1-9 (1984).
38. Tzamtzis, A. "Finite element modeling of cracks and joints in discontinuous structural systems", In *The 16th ASCE Engineering Mechanics Conference*, Seattle (2003).
39. Rocscience Inc., Phase² v7.0 - *Two-Dimensional Finite Element Slope Stability Analysis*, Toronto (2007).
40. Timoshenko, S. and Goodier, J.N., *Theory of Elasticity*, 3-D Ed., New York, McGraw-Hill (1970).

APPENDIX

Derivation of Constitutive Equations

For the derivation of the components of the elasticity tensor, an equivalent continuum concept is applied, in which it is assumed that the intact material comprising the layers and interfaces interacts similar to a number of springs in series [36]. Using a characteristic volume that is sufficiently large compared to the internal characteristic length (the layer thickness), the elasticity matrix of the classical equivalent continuum of Figure 2d is obtained as follows:

$$\widehat{\mathbf{D}} = \begin{pmatrix} \widehat{\mathbf{D}}_n & \mathbf{0} \\ \mathbf{0} & \widehat{\mathbf{D}}_s \end{pmatrix},$$

$$D_n = \begin{pmatrix} 1/E & -\nu/E & -\nu/E \\ -\nu/E & 1/E & 1/E \\ -\nu/E & -\nu/E & 1/E \end{pmatrix},$$

$$D_s = \begin{pmatrix} 1/G + 1/hk_s & 0 & 0 \\ 0 & 1/G + 1/hk_s & 0 \\ 0 & 0 & 1/G \end{pmatrix}. \quad (\text{A1})$$

In the Cosserat continuum, shear stresses are not symmetric. Also, in addition to the true stress tensor, a couple-stress tensor is assumed to exist at each point of the material.

In order to derive the additional Cosserat parameters of a layered medium with a sequential microstructure, the mechanical model of a stack of interacting plates is considered. Figure 2d shows the characteristic

volume of a Cosserat layered material and the non-zero stress and couple stress measures acting on it. The mechanical response of each layer of the material is similar to a plate. A single thin plate, with a normal vector, $\widehat{\mathbf{e}}_3$, is shown in Figure 2e.

The mechanical behavior of a plate can be represented by the following assumptions:

$$\widehat{\theta}_1 \neq 0, \quad \widehat{\theta}_2 \neq 0, \quad \widehat{\theta}_3 = 0. \quad (\text{A2})$$

A direct consequence of the assumptions expressed by Equation A2 is that all curvature measures corresponding to $\widehat{\theta}_3$ can be neglected:

$$\widehat{\kappa}_{31} = \widehat{\kappa}_{32} = \widehat{\kappa}_{33} = 0. \quad (\text{A3})$$

In plate theory, in addition to the bending moments, twisting moments need to be accounted for [34]. The curvature changes to the deflected middle surface of a plate are expressed by:

$$k_x = -\frac{\partial^2 w}{\partial x^2}, \quad k_y = -\frac{\partial^2 w}{\partial y^2},$$

and:

$$\chi = -\frac{\partial^2 w}{\partial x \partial y}, \quad (\text{A4})$$

where w is the deflection and χ represents the warping of the plate, and is equal to zero if the twisting mechanism is neglected. In the Cosserat formulation of materials with plate-like microstructures, the curvature measures due to the twisting of the section are represented by $\widehat{\theta}_{i,i}$, while the curvature measures due to the bending are represented by $\widehat{\theta}_{i,j}$.

Considering the mechanics of a plate depicted in Figure 2e, it can be interpreted that part of each shear stress component across the thickness of the layer, e.g. $\widehat{\sigma}_{13}$, is in equilibrium with its conjugate shear component, i.e. $\widehat{\sigma}_{31}$, and is related to the corresponding strain components through the shear coefficient of the equivalent continuum, G_{11} , expressed by:

$$\widehat{\sigma}_{31} = G_{11}(\widehat{\gamma}_{13} + \widehat{\gamma}_{31}),$$

$$\widehat{\sigma}_{32} = G_{11}(\widehat{\gamma}_{23} + \widehat{\gamma}_{32}), \quad (\text{A5})$$

with:

$$G_{11} = 1 / \left(\frac{1}{G} + \frac{1}{hk_s} \right) = \frac{Ghk_s}{G + hk_s},$$

where h is the layer thickness, k_n and k_s are the normal and shear stiffness of the interface, and G is the shear modulus of the intact material. However, the stress occurring across the thickness of the layer has a

contribution from the bending of the layers, which is related to $\widehat{\gamma}_{13}$ through the shear modulus of the intact material comprising the individual layers, i.e. G . Thus, the stress component in the direction of the layers can then be expressed as:

$$\begin{aligned}\widehat{\sigma}_{13} &= G_{11}(\widehat{\gamma}_{13} + \widehat{\gamma}_{31}) + G\widehat{\gamma}_{13}, \\ \widehat{\sigma}_{23} &= G_{11}(\widehat{\gamma}_{23} + \widehat{\gamma}_{32}) + G\widehat{\gamma}_{23}.\end{aligned}\quad (\text{A6})$$

In the Cosserat theory, the couple-stress measures or micromoments also need to be defined with respect to their work conjugate curvature measures. Using the mechanics of a single plate element, it can be concluded that the non-zero couple stress measures in a layered medium, represented in Figure 2d, are $\widehat{\mu}_{21}$ and $\widehat{\mu}_{12}$, which are due to the bending mechanism, and $\widehat{\mu}_{11}$ and $\widehat{\mu}_{22}$, which are due to the twisting mechanism. The non-zero bending couple stresses, $\widehat{\mu}_{21}$ and $\widehat{\mu}_{12}$, can be related to the curvature of the system through the bending stiffness of the interacting layers as follows:

$$\widehat{\mu}_{12} = B(\widehat{\kappa}_{12} + \nu\widehat{\kappa}_{21}), \quad (\text{A7})$$

and:

$$\widehat{\mu}_{21} = B(\widehat{\kappa}_{21} + \nu\widehat{\kappa}_{12}),$$

with:

$$B = \frac{Eh^2}{12(1-\nu^2)} \left(\frac{G - G_{11}}{G + G_{11}} \right),$$

where ν is the Poisson ratio of the intact material comprising the layers and reflects the Poisson effect on the bending moments. The curvature measures, $\widehat{\kappa}_{11}$ and $\widehat{\kappa}_{22}$, are analogous with the curvature measure, χ , in plate theory. Thus, the twisting couple stresses are related to their corresponding curvature measures through:

$$\mu_{11} = (1 - \nu)B(\widehat{\kappa}_{11}), \quad (\text{A8})$$

and:

$$\mu_{22} = (1 - \nu)B(\widehat{\kappa}_{22}).$$

Using the above arguments and assuming isotropic behavior for the individual plate, $\widehat{\mathbf{D}}_1$ and $\widehat{\mathbf{D}}_2$ are expressed by Equations 21-24. It should be noted that coefficients of A_{ij} and G_{11} are similar to those in a classical transversely isotropic material expressed by Equation A1, while the additional Cosserat parameters are G_{22} and B , which incorporate the effect of non-symmetrical stresses and the bending stiffness of the layers. Two limit cases are of special interest: first, if plates are non-interacting, then $k_n \rightarrow \infty$ and $k_s \rightarrow 0$, and the bending stiffness of the system is equal to the sum of the bending stiffness of the individual layers; second, in the case where $k_s \rightarrow \infty$, the second parenthesis of B , expressed by Equation A7, will approach zero, and the effect of bending stiffness vanishes. In this case, the Cosserat formulation reduces to the classical continuum formulation.

Finally, the local constitutive matrices, $\widehat{\mathbf{D}}_1$ and $\widehat{\mathbf{D}}_2$, should be expressed in the global coordinate system using the transformation rules of fourth-rank tensors. It should be noted that in a 2-D analysis, the local coordinates of the Cosserat rotation always coincide with the out-of-plane axis of the global coordinate system. However, in a 3-D analysis of an arbitrarily-orientated plate or beam, in spite of the simplifications involved in the 3-D formulation of Cosserat rotations in the local coordinate system, generally the projection of the rotation vector on the global coordinates results in 3 components. Consequently, for an arbitrarily-orientated plate or beam, all 9 components of the curvature tensor should be preserved in the FEM formulation.